

## Mode coupling in a He-Ne ring laser with backscattering

R. J. C. Spreeuw, R. Centeno Neelen, N. J. van Druten, E. R. Eliel, and J. P. Woerdman  
*Huygens Laboratory, University of Leiden, P.O. Box 9504, 2300 RA Leiden, The Netherlands*

(Received 18 May 1990)

An alternative approach is proposed to discuss mode coupling in bidirectional ring lasers that is induced by backscattering. It is shown that various features can be simply discussed in terms of the mode structure of the corresponding *passive* ring cavity. The nature of the backscattering is found to play a crucial role in determining the normal-mode structure. For instance, we show theoretically that, for a rotating ring laser (gyro), the characteristics of frequency locking are already present in the passive-mode structure if the mode coupling has a dissipative nature, i.e., if the backscattering originates in localized losses. If, on the other hand, the backscattering has a conservative nature, i.e., originates in steps of the refractive index, a frequency splitting is found in the passive-mode structure, making so-called oscillatory instability possible. Experimental observations are reported to support this point of view. The recently reported  $\pi$ -phase jumps in He-Ne ring lasers are shown to fit naturally into this scheme. These jumps can be described as transitions between the normal modes of the passive ring cavity.

### I. INTRODUCTION

The behavior of the counterpropagating traveling waves in ring lasers in the presence of backscattering has been the subject of many papers.<sup>1-14</sup> The backscattering produces a linear coupling of the clockwise (cw) and counterclockwise (ccw) propagating waves. Additionally, since we deal with a laser, the two modes are nonlinearly coupled by the saturation of the gain medium. The interest in these phenomena stems partly from the field of ring-laser gyroscopes where backscattering gives rise to locking at low rotation rates.<sup>1-7</sup> Interest has also been generated by the statistical properties of ring lasers with backscattering or by their nonlinear dynamics.<sup>8-14</sup> Interesting features have been discovered, such as oscillatory instabilities<sup>2,7,11,13,14</sup> and phase jumps.<sup>10,11,13</sup>

It is our aim here to show that, although a full analysis of these systems leads inevitably into the field of nonlinear dynamics, many features in ring-laser behavior may conveniently be discussed in the context of the mode structure of the passive ring cavity.<sup>7,14,17</sup> This involves, essentially, solving an eigenvalue problem and performing a transformation towards the basis of passive eigenmodes. As an example, a coupling term (backscattering) that arises in one basis may appear as a frequency shift in a different basis.

We feel that the convenience of this approach has been insufficiently appreciated so far. It is particularly useful when the linear coupling by the backscattering dominates the nonlinear coupling by the gain medium. This situation occurs naturally when the cross-saturation of the counterpropagating modes equals the self-saturation, so that the mode competition is neutral. A single Ne-isotope He-Ne ring laser tuned to line center comes very close to this condition<sup>9</sup> and we report in this paper, apart from the theoretical discussion, some experimental results on backscattering-induced mode-coupling phenomena in such a laser. Related work on ring dye lasers will

be published elsewhere.<sup>14</sup>

Our theoretical approach is presented in Sec. II. We show in Sec. III that, depending on the nature of the backscattering, the mode structure of a passive rotating ring cavity may display either frequency locking or frequency repulsion. Some implications for the performance of a laser gyro are considered. The well-known oscillatory instabilities in (nonrotating) ring lasers with backscattering are described in Sec. IV in terms of normal-mode frequency splittings. In Sec. V we present a novel interpretation of the so-called  $\pi$ -phase jumps. In Sec. VI experimental results on the oscillatory instability will be presented; these support the point of view that the instability can be seen as a normal-mode frequency splitting. Conclusions are given in Sec. VII.

### II. LINEAR MODE-COUPLING ANALYSIS

Within the context of third-order laser theory, the behavior of a (single-mode) ring laser is described quite adequately by a set of nonlinear equations of motion for the counterpropagating wave amplitudes. We assume zero detuning from line center (i.e., we disregard self- and cross-pushing and -pulling effects) and give the equations in dimensionless form:<sup>9,14</sup>

$$\dot{\tilde{E}}_1 = -i(\tilde{K}_{11}\tilde{E}_1 + \tilde{K}_{12}\tilde{E}_2) - (|\tilde{E}_1|^2 + \xi|\tilde{E}_2|^2)\tilde{E}_1, \quad (1a)$$

$$\dot{\tilde{E}}_2 = -i(\tilde{K}_{21}\tilde{E}_1 + \tilde{K}_{22}\tilde{E}_2) - (|\tilde{E}_2|^2 + \xi|\tilde{E}_1|^2)\tilde{E}_2, \quad (1b)$$

Here  $\tilde{E}_1$  and  $\tilde{E}_2$  are the complex amplitudes of the clockwise and counterclockwise propagating waves,  $\xi$  is the ratio of the cross- and self-saturation coefficients ( $0 \leq \xi \leq 2$ ), and the numbers  $\tilde{K}_{ij}$  constitute a  $2 \times 2$  complex dynamical matrix describing the linear part of the evolution. The equations are essentially the same as those used by other authors;<sup>3,8,9</sup> our notation is somewhat unconventional in order to stress the connection

with the eigenvalue problem of the passive cavity. Unless explicitly stated otherwise, we shall retain the dimensionless form of the equations throughout this paper.

In general the nonlinear equations have to be integrated numerically. Here we restrict ourselves to situations where the mode structure of the passive cavity provides a convenient framework for discussing ring-laser behavior. Therefore we first consider the linear part of Eqs. (1a) and (1b), determine the eigenmodes and then consider the nonlinear terms, which give rise to competition between the eigenmodes of the linear system. The linear part of Eqs. (1a) and (1b) can be considered as a coupled oscillator model for the counterpropagating waves<sup>4</sup> and can be written as

$$\frac{d}{dt} \begin{pmatrix} \tilde{E}_1 \\ \tilde{E}_2 \end{pmatrix} = -i\tilde{K} \begin{pmatrix} \tilde{E}_1 \\ \tilde{E}_2 \end{pmatrix}. \quad (2)$$

The eigenmodes of the linear system are now given by the eigenvectors of the dynamical matrix  $\tilde{K}$ . The real and imaginary parts of the corresponding eigenvalues give the frequencies and damping rates of the modes. Note that in this  $2 \times 2$  matrix description it is implicitly assumed that the two modes under consideration are well isolated from other cavity modes. Stated differently, the frequency difference between the modes as determined by  $\tilde{K}$  must be small as compared to the free spectral range of the ring cavity.

For an interpretation of the physics underlying the matrix elements  $\tilde{K}_{ij}$  it is instructive to decompose  $\tilde{K}$  into its Hermitian and anti-Hermitian parts:

$$\tilde{K} = \frac{1}{2}(\tilde{K} + \tilde{K}^\dagger) + \frac{1}{2}(\tilde{K} - \tilde{K}^\dagger) \equiv \tilde{H} + i\tilde{A}, \quad (3)$$

where a dagger<sup>†</sup> denotes Hermitian conjugation. Since  $\tilde{H}$  and  $\tilde{A}$  are now both Hermitian, their eigenvalues will be real. The form of Eq. (3) suggests that  $\tilde{H}$  contains conservative mechanisms, i.e., mechanisms that merely redistribute energy between different modes. Conversely,  $\tilde{A}$  may be interpreted as containing all dissipative mechanisms, including linear gain.

The diagonal elements of  $\tilde{H}$  and  $\tilde{A}$  represent the frequencies and damping rates, respectively, of the traveling wave modes in the absence of coupling. A frequency difference between the uncoupled cw and ccw waves may be caused by a nonreciprocal phase, e.g., the Sagnac effect in a ring-laser gyroscope, or the Faraday effect.<sup>16-18</sup> A difference in damping rate between cw and ccw waves occurs, for example, in ring dye lasers equipped with a unidirectional device.

The off-diagonal elements of  $\tilde{H}$  and  $\tilde{A}$  represent coupling between the cw and ccw waves due to backscattering. We shall call the coupling produced by  $\tilde{H}$  "conservative" and that by  $\tilde{A}$  "dissipative." With the term conservative we adhere to the definition given by Haus, Statz and Smith.<sup>5</sup> An alternative, widely used, terminology is "off-phase" for conservative and "in-phase" for dissipative.<sup>8,12</sup> The difference between these two kinds of backscattering becomes clear in the following examples. Let us consider a dynamical matrix where the only nonzero components are the off-diagonal elements of either  $\tilde{H}$  or  $\tilde{A}$ :

$$\tilde{K} = \beta \begin{pmatrix} 0 & We^{i\phi} \\ We^{-i\phi} & 0 \end{pmatrix}, \quad (4)$$

where  $W$  is a dimensionless backscattering rate (real and positive) and  $\beta=1$  or  $i$  for conservative or dissipative backscattering, respectively. The phase  $\phi$  is determined by the position of the backscatterer relative to a chosen reference plane and is not essential for the results to be obtained. We shall therefore set  $\phi=0$  throughout this paper. The results for arbitrary  $\phi$  may be found by multiplying the cw component of the eigenvectors by  $e^{i\phi/2}$  and the ccw component by  $e^{-i\phi/2}$ . In view of the spatial dependence of the cw and ccw waves ( $\sim e^{ikz}$  and  $\sim e^{-ikz}$ ), this is essentially a displacement along the beam axis. Irrespective of the type of backscattering (i.e., the value of  $\beta$ ), the eigenvectors of  $\tilde{K}$  are

$$\frac{1}{\sqrt{2}} \begin{pmatrix} 1 \\ 1 \end{pmatrix}, \quad \frac{1}{\sqrt{2}} \begin{pmatrix} -1 \\ 1 \end{pmatrix}. \quad (5)$$

The corresponding eigenvalues are  $\pm\beta W$ . Since the cw and ccw amplitudes are equal in magnitude, the eigenvectors represent standing waves. The two eigenvectors are orthogonal, which expresses the spatial complementarity of the standing waves: the nodes of one standing wave coincide with the antinodes of the other. For the conservative case the eigenvalues are real, so that the standing waves have different frequencies. For the dissipative case, we find imaginary eigenvalues, i.e., different loss rates. (We actually find one mode with gain, so that in a passive system  $\tilde{K}$  must contain an additional loss term.)

The two types of backscattering may arise from localized steps in the refractive index or in the absorption coefficient for the conservative and dissipative case, respectively. By "localized" we refer to spatial variation on a scale smaller than a wavelength. A similar distinction is made in Refs. 3 and 5. In the context of distributed feedback media, the same distinction appears between "index coupling" (conservative) and "gain coupling" (dissipative).<sup>7,19</sup> We shall give a simple example of both types of backscattering.

Consider, as a first example, a plane-parallel plate, made from a lossless dielectric, aligned perpendicular to the mode axis in a ring-resonator cavity. This element evidently gives rise to backward reflection and thus couples the counterpropagating waves. Since the dielectric is lossless, the plate can only redistribute intensity between the two directions of propagation and must therefore be a conservative scatterer. It was shown in earlier work that such a backscattering element gives normal modes that are standing waves, with a frequency difference determined by the effective reflection coefficient of the backscatterer.<sup>7,15,16,18</sup> Using a transmission matrix formalism,<sup>18</sup> it can be shown that the low-frequency mode has an antinode in the center of the dielectric plate and the high-frequency mode has a node. This suggests an interpretation of the frequency difference as a difference in dielectric polarization energy.<sup>7</sup>

In our second example we replace the plate by a localized absorber, e.g., an absorbing layer, thin as compared to a wavelength, perpendicular to the mode axis. It can

be shown that Mie scattering by a dust particle somewhere along the resonator (e.g., on one of the mirrors) may serve the same purpose.<sup>5</sup> If we consider two standing waves, one with a node at the absorber and the other with an antinode, it is clear that the former experiences no loss (ideally), whereas the latter has maximum loss. Apart from an overall loss rate, these standing waves are exactly the eigenmodes of the matrix in Eq. (4) with  $\beta=i$ . We may convince ourselves of the scattering mechanism inherent to localized absorption (or gain), by considering a traveling wave, clockwise say, that is present at a certain time inside the cavity. Alternatively this traveling wave may be seen as a superposition of the standing waves just discussed. The standing-wave component with an antinode at the absorber will decay, whereas the standing wave with a node at the absorber remains undamped. The remaining standing wave can, in its turn, be seen as a superposition of cw and ccw traveling waves. Since in the overall process part of the initial cw traveling wave has been converted to a ccw traveling wave, localized absorption clearly implies a scattering mechanism.

A more formal argument shows that the presence of orthogonal standing-wave eigenmodes (e.g., imposed by symmetry) already implies a scattering mechanism, provided that the (complex) eigenvalues are different. In the standing-wave eigenbasis the dynamical matrix is now evidently diagonal. A unitary transformation to a basis of traveling waves then yields a dynamical matrix with nonzero off-diagonal elements which represent backscattering. One may verify that the magnitude of the obtained backscattering rate is equal to  $|\tilde{\lambda}|$ , where  $2\tilde{\lambda}$  is the difference between the complex eigenvalues. In other works, the traceless part of  $\tilde{K}$  takes the form of Eq. (4), with  $\beta W$  replaced by  $\tilde{\lambda}$  and with  $\beta=e^{i\psi}$  somewhere on the unit circle in the complex plane. The coupling thus found is therefore in general intermediate between conservative and dissipative. Such a coupling may clearly be realized by using an intracavity étalon, made from a material with a complex refractive index, again perpendicular to the mode axis. The full range from conservative to dissipative coupling can also be realized by using two extracavity backreflectors.<sup>8-10,13</sup>

### III. BACKSCATTERING IN ROTATING RING CAVITIES

Frequency locking in ring-laser gyroscopes is generally attributed to backscattering. However, in treatments of laser gyroscopes, conservative and dissipative backscattering are rarely distinguished in their effect on locking behavior. By solving the eigenvalue problem as defined in Sec. II, we shall show here that the nature of the backscattering strongly determines the passive-mode structure. Subsequently we shall consider some implications for the performance of an active (laser) gyro.

Restricting ourselves to the extreme cases of purely conservative and purely dissipative coupling, we write the dynamical matrix in the form

$$\tilde{K} = \begin{pmatrix} S & \beta W \\ \beta W & -S \end{pmatrix}. \quad (6)$$

Here  $2S$  is the rotation-induced frequency splitting between the cw and ccw modes in the absence of backscattering (Sagnac effect), and  $\beta$  and  $W$  are defined as in Eq. (4). Note that we have chosen the zero of our frequency scale in such a way that  $\tilde{K}$  is traceless.

The parameters in Eq. (6) are defined as dimensionless quantities. The actual dimensions are retrieved if we replace  $W$  by  $rc/L$ , where  $L/c$  is the cavity round-trip time and  $r$  is the fractional amount of backscattering per round-trip (i.e., the effective amplitude-reflection coefficient), with  $r \ll 1$  in view of the validity of the two-mode approach. The dimensionless frequency splitting  $2S$  must then be replaced by the actual splitting produced by the Sagnac effect, in units of angular frequency. The resulting eigenvalues of  $\tilde{K}$  are then obtained as angular frequencies.

#### A. Frequency locking by dissipative backscattering

For dissipative coupling ( $\beta=i$ ) we find for the eigenvalues  $\tilde{\lambda}=\pm(S^2-W^2)^{1/2}$ , i.e., real values for  $|S| \geq W$  and imaginary values for  $|S| \leq W$ . The frequency splitting, which depends linearly on  $S$  in an ideal gyro, is reduced by the backscattering and vanishes below a critical rotation rate, thus defining a locking region:  $|S| \leq W$ ; see Fig. 1(a). The width of the locking region ( $2W$ ) is proportional to the amplitude backscattering rate. We thus recognize the familiar locking behavior of a laser gyro already in the passive cavity mode structure, if the backscattering is dissipative.

One must realize that the eigenmodes of a rotating laser gyro with dissipative backscattering are generally not orthogonal. Inside the locking region ( $|S| < W$ ) the eigenvectors of Eq. (6) have equal frequencies but different damping rates and represent standing waves:

$$\frac{1}{\sqrt{2}} \begin{pmatrix} ie^{i\alpha} \\ e^{-i\alpha} \end{pmatrix}, \quad \frac{1}{\sqrt{2}} \begin{pmatrix} ie^{-i\alpha} \\ e^{i\alpha} \end{pmatrix}, \quad (7)$$

with  $\cos 2\alpha = -S/W$ . Note that  $2\alpha$  is essentially the phase difference of the cw and ccw components. This dependence of  $2\alpha$  on the rotation rate is well known for laser gyros in the locked regime, where only one standing

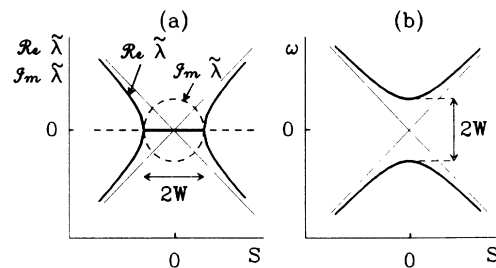


FIG. 1. Eigenmode frequencies (thick solid line;  $\text{Re } \tilde{\lambda}$  and  $\omega$ ) and damping rates (dashed line;  $\text{Im } \tilde{\lambda}$ ) of passive rotating ring resonators. In both cases  $S$  is the rotation rate and  $W$  the backscattering rate. In (a) the backscattering is dissipative; locking occurs for  $|S| < W$ . In (b) the backscattering is conservative and the modes are undamped.

wave is present.<sup>6</sup> Physically this means that the position of the standing wave is shifted along the ring when the ring is set into rotation. The maximum position shift is reached at the locking threshold ( $|S|=W$ ) and equals  $\lambda/8$ , where  $\lambda$  is the wavelength. The scalar product of the eigenvectors (overlap of the modes) is equal to  $-S/W$ , so that the modes are orthogonal for zero rotation rate and become identical when the locking threshold is reached ( $|S|=W$ ). Outside the locking region ( $|S|>W$ ), the eigenvectors have equal damping rate but different frequencies and are given by

$$N \begin{bmatrix} i \cosh\chi \\ \sinh\chi \end{bmatrix}, \quad N \begin{bmatrix} i \sinh\chi \\ \cosh\chi \end{bmatrix}, \quad (8)$$

where  $\coth 2\chi = -S/W$  and  $N = 1/\sqrt{\cosh 2\chi}$  is a normalization factor. The scalar product of the eigenvectors is now  $-W/S$ , so that far from the locking threshold ( $|S| \gg W$ ) the modes approach their asymptotic forms of cw and ccw traveling waves and become orthogonal. Again, the modes become identical upon approaching the locking threshold ( $|S| \searrow W$ ).

For a complete description the nonlinear coupling in the gain medium must be taken into account. This is required, e.g., to explain the anharmonic beat signals occurring just above the locking threshold.<sup>1,6,8,14</sup> Note that such a description is also complicated by the nonorthogonality of the modes. A complete description therefore remains a complicated problem. What we want to stress here, is that locking characteristics are a property of the *passive* ring cavity if the backscattering is dissipative. The assumption of a dissipative contribution to the backscattering seems reasonable for actual laser gyroscopes, where it may originate in dust particles and scattering losses in the mirrors.

### B. Frequency repulsion by conservative backscattering

For conservative coupling ( $\beta=1$ ) we always find real eigenvalues of  $\vec{K}$  [Eq. (6)]:  $\tilde{\lambda} = \omega = \pm(S^2 + W^2)^{1/2}$ . In contrast with the dissipative case of Sec. III A, the difference between the eigenfrequencies is now larger than in the absence of backscattering ( $W=0$ ). The dependence of the eigenfrequency on the rotation rate  $S$  shows an avoided crossing [Fig. 1(b)] with a minimum separation given by  $2W$ . For the eigenvectors we find

$$\begin{bmatrix} \cos\theta \\ \sin\theta \end{bmatrix}, \quad \begin{bmatrix} -\sin\theta \\ \cos\theta \end{bmatrix}, \quad (9)$$

with  $\cot 2\theta = S/W$ . The eigenvectors are orthogonal as a consequence of the Hermiticity of  $\vec{K}$ . Note that for a nonrotating cavity ( $S=0$ ), the corresponding eigenmodes are standing waves, as was shown already in Sec. II. With increasing rotation rate the eigenmodes gradually approach their asymptotic forms, i.e., cw and ccw traveling waves.

In a ring laser, the nonlinear interaction of the waves in the gain medium leads to competition between the passive normal modes. For the laser gyro with conservative backscattering two possibilities exist in the limit of low rotation rate ( $|S| \ll W$ ). The laser may either oscillate simultaneously in both normal modes (approximately

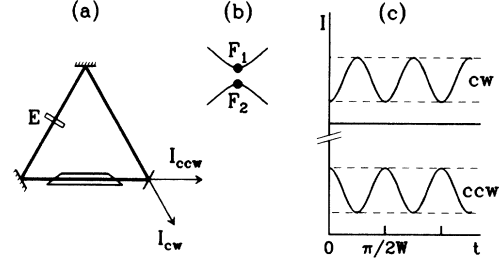


FIG. 2. Ring laser (a) with conservative backscatterer  $E$ , oscillating in the two standing-wave modes of Fig. 1(b) in the absence of rotation ( $S=0$ ). The corresponding normal-mode frequency diagram is shown in (b) with standing-wave amplitudes  $F_1$  and  $F_2$ . The beat frequency of the standing waves ( $2W$ ) corresponds to intensity modulation of the traveling waves, so-called oscillatory instability (c). The cw and ccw intensities  $I_{cw}$  and  $I_{ccw}$  are oscillating in antiphase between the levels  $(F_1 - F_2)^2/2$  and  $(F_1 + F_2)^2/2$ . These levels are shown as dashed lines.

standing waves), or in only one, depending on whether the competition between the standing waves is weak or strong.<sup>3</sup> In the former case we observe cw and ccw intensities that are modulated at the beat frequency ( $\approx 2W$  for low rotation rate, see Fig. 2), whereas in the latter case no beat is present.<sup>14</sup> In Sec. IV we discuss which situation actually occurs for different gain media.

From an operational point of view, laser oscillation in a single normal mode, as may occur here due to conservative backscattering, is difficult to distinguish from frequency locking due to dissipative backscattering. In both cases the beat note of the laser gyro disappears for low rotation rates. In fact, according to the definition of locking in Ref. 5, i.e., a situation in which the phase difference between the traveling waves is constant in time, both situations are actually called locking. This result contradicts the statement in Ref. 5 that conservative backscattering does *not* lead to locking. This statement is based on the commonly made assumption that the amplitudes of the counterpropagating waves are equal. Let us examine the validity of this assumption by considering first a laser oscillating in a single normal mode. In this case we expect from Eq. (9) that the cw and ccw amplitudes are generally different and equal only for zero rotation rate ( $S=0$ ). In the other possible case, where the laser oscillates simultaneously in both normal modes, the counterpropagating intensities are modulated in antiphase at the beat frequency (see also Sec. IV), so that they are evidently unequal. We conclude therefore, that the common assumption of equal amplitudes is not justified and leads to incorrect results. Also conservative backscattering can lead to locking.

The linear two-mode analysis as presented in this section is valid as long as the two modes are well isolated from other longitudinal modes. In other words, the frequency splittings produced by  $W$  and  $S$  must be small as compared to the free spectral range of the ring cavity. The complete mode structure of a rotating ring resonator

with conservative backscattering, containing all longitudinal modes, can be obtained from a transmission matrix formalism and leads to an optical band structure.<sup>15-18</sup> The mode frequencies, expressed in units of angular frequency (i.e., not dimensionless), are then given by

$$\omega = \frac{c}{L} \{2\pi q \pm \arccos[(1-r^2)^{1/2} \cos \phi_S]\} . \quad (10)$$

Here  $c/L$  is the free spectral range of the cavity,  $q$  is an integer (the cavity mode number),  $r$  is the amplitude-reflection coefficient of the backscatterer, and  $\phi_S$  is the nonreciprocal (Sagnac) phase per round-trip. The longitudinal mode splitting (for fixed  $q$ ) reduces to the two-mode result when  $r$  and  $\phi_S$  are small ( $r, \phi_S \ll 1$ ):  $\Delta\omega \approx (2c/L)(r^2 + \phi_S^2)^{1/2}$ . A similar extension may be made for the dissipative case.

#### IV. OSCILLATORY INSTABILITY

Oscillatory instabilities in (nonrotating) ring lasers with backscattering were reported for several laser systems.<sup>2,7,11,13,14</sup> In the time domain they can be described with an oscillatory cross-correlation function for the traveling-wave intensities.<sup>10</sup> We shall give here a description in the frequency domain that is conceptually simpler. We describe the phenomenon as a stable operation in two standing waves, the eigenmodes of the passive cavity (Fig. 2). The nonlinearity associated with gain saturation of the laser medium leads to mode competition between the passive eigenmodes.

We shall restrict ourselves to the situation where the backscattering is equally strong in both directions, but intermediate between dissipative and conservative. The dynamical matrix for this situation may be written as

$$\bar{K} = \begin{pmatrix} ia & \beta W \\ \beta W & ia \end{pmatrix}, \quad (11)$$

where we have set  $S=0$  (nonrotating ring laser) and where  $a$  is the (dimensionless) pump parameter, i.e., the amount of unsaturated gain minus loss (cf. Ref. 9). We assume the pump parameter to be real and equal for both traveling waves, which is correct for zero detuning from line center. The parameter  $\beta = e^{i\psi}$  determines the nature of the backscattering, with  $\sin\psi=0$  for conservative and  $\cos\psi=0$  for dissipative backscattering. The backscattering rate  $W$  is real and positive as before. The eigenvalues are  $ia \pm W e^{i\psi}$  with eigenvectors given by Eq. (5). We thus find two orthogonal standing-wave modes with a frequency splitting  $2W \cos\psi$  and a difference in damping rate  $2W \sin\psi$ . For  $\cos\psi=0$  the backscattering is dissipative and the difference in frequency vanishes. On the other hand, the difference in damping rate vanishes for  $\sin\psi=0$  or conservative backscattering. We now choose the standing-wave normal modes of Eq. (5) as a basis for our two-mode problem, i.e., we express the field in the complex standing-wave amplitudes  $\bar{F}_1$  and  $\bar{F}_2$  through the transformation

$$\begin{aligned} \begin{pmatrix} \bar{E}_1 \\ \bar{E}_2 \end{pmatrix} &= \frac{\bar{F}_1}{\sqrt{2}} \begin{pmatrix} 1 \\ 1 \end{pmatrix} + \frac{\bar{F}_2}{\sqrt{2}} \begin{pmatrix} -1 \\ 1 \end{pmatrix} \\ &= \frac{1}{\sqrt{2}} \begin{pmatrix} 1 & -1 \\ 1 & 1 \end{pmatrix} \begin{pmatrix} \bar{F}_1 \\ \bar{F}_2 \end{pmatrix}. \end{aligned} \quad (12)$$

In order to describe competition between the modes  $\bar{F}_{1,2}$  we must return to the nonlinear equations (1a) and (1b). With Eq. (12) and the coefficients  $\bar{K}_{ij}$  from Eq. (11), Eqs. (1a) and (1b) are transformed into the following evolution equations for the standing-wave amplitudes:<sup>3,12</sup>

$$\begin{aligned} \dot{\bar{F}}_1 &= \left[ a - iW e^{i\psi} - \frac{1+\xi}{2} |\bar{F}_1|^2 - |\bar{F}_2|^2 \right] \bar{F}_1 \\ &\quad + \frac{\xi-1}{2} (\bar{F}_1^* \bar{F}_2) \bar{F}_2, \end{aligned} \quad (13a)$$

$$\begin{aligned} \dot{\bar{F}}_2 &= \left[ a + iW e^{i\psi} - \frac{1+\xi}{2} |\bar{F}_2|^2 - |\bar{F}_1|^2 \right] \bar{F}_2 \\ &\quad + \frac{\xi-1}{2} (\bar{F}_1 \bar{F}_2^*) \bar{F}_1, \end{aligned} \quad (13b)$$

where the asterisk \* denotes complex conjugation. We may now introduce  $a_{1,2} \equiv a \pm W \sin\psi$  as the effective pump parameters for the standing waves and  $\Omega_{1,2} \equiv \pm W \cos\psi$  as the frequencies of the standing waves. If we assume  $\xi=1$  (which is generally found to describe a single Ne-isotope He-Ne ring laser tuned to line center<sup>9</sup>), these equations reduce to

$$\dot{\bar{F}}_1 = (a_1 - i\Omega_1 - |\bar{F}_1|^2 - |\bar{F}_2|^2) \bar{F}_1, \quad (14a)$$

$$\dot{\bar{F}}_2 = (a_2 - i\Omega_2 - |\bar{F}_2|^2 - |\bar{F}_1|^2) \bar{F}_2. \quad (14b)$$

We see that only the sum of the intensities  $|\bar{F}_1|^2 + |\bar{F}_2|^2$  appears as a saturation term, so that the degree of saturation is equal for both modes, i.e., mode competition is neutral.

If, additionally, the coupling is conservative, we have  $\sin\psi=0$ , so that  $a_1=a_2=a$  and  $\Omega_1=-\Omega_2=W$  (choosing  $\cos\psi=+1$ ). This leads to the following stationary solutions of Eqs. (14a) and (14b), up to constant phase factors:

$$\bar{F}_1(t) = F_1 e^{-iWt}, \quad (15a)$$

$$\bar{F}_2(t) = F_2 e^{iWt}, \quad (15b)$$

with  $F_1$  and  $F_2$  chosen as real and positive and  $F_1^2 + F_2^2 = a$ . As a consequence of the neutral character of the mode competition ( $\xi=1$ ), this stationary solution is indifferent with respect to a redistribution of the intensity between the modes  $\bar{F}_1$  and  $\bar{F}_2$ . We will come back to this point in Sec. V A. Transforming the solutions Eqs. (15a) and (15b) back to the traveling-wave basis, we find for the cw and ccw amplitudes

$$\bar{E}_1(t) = \frac{1}{\sqrt{2}} [(F_1 - F_2) \cos Wt - i(F_1 + F_2) \sin Wt], \quad (16a)$$

$$\bar{E}_2(t) = \frac{1}{\sqrt{2}} [(F_1 + F_2) \cos Wt - i(F_1 - F_2) \sin Wt]. \quad (16b)$$

The cw and ccw intensities  $|\tilde{E}_1(t)|^2$  and  $|\tilde{E}_2(t)|^2$  will therefore be modulated in antiphase at a frequency  $2W$ , with a modulation depth determined by  $\frac{1}{2}(F_1 - F_2)^2$  and  $\frac{1}{2}(F_1 + F_2)^2$ ; see Fig. 2. This behavior, which was called “oscillatory instability” or “intensity oscillation” by several authors,<sup>2,7-11,13,14</sup> corresponds in our picture with a stable operation in two standing-wave modes.

Oscillatory instability was also observed in ring-laser systems for which the condition  $\xi=1$  is not met. We can see from Eqs. (13a) and (13b) that the ratio of the cross- and self-saturation coefficients for the *standing* waves is equal to  $2/(1+\xi)$ . Therefore weak competition between traveling waves ( $\xi < 1$ ) leads to strong competition between standing waves [ $2/(1+\xi) > 1$ ] and vice versa. Note that we disregard the influence of the last terms in Eqs. (13a) and (13b), since they vary rapidly in time. It is shown in Ref. 14 that these terms do not influence the character (i.e., strong or weak) of the mode competition.<sup>20</sup> For oscillatory instability we need weak (or neutral) competition between standing waves, or  $\xi \geq 1$ . Ring lasers with a homogeneously broadened gain medium, such as dye ring lasers, satisfy this condition ( $\xi=2$ ) and therefore show oscillatory instability.<sup>8,14</sup> Ring lasers for which  $\xi < 1$ , such as a He-Ne ring laser with an isotopic mixture of <sup>20</sup>Ne and <sup>22</sup>Ne, have not been observed to show oscillatory instability. These lasers oscillate instead in one standing-wave mode, as was observed in ring-laser gyros.<sup>1,3</sup>

## V. $\pi$ -PHASE JUMPS

The applicability of our linear two-mode analysis to a ring laser with backscattering is determined by the relative strength of the linear coupling as compared to that of the nonlinear coupling. We may expect our approach to be useful in those cases where the linear coupling dominates. As mentioned already in Sec. IV, the nonlinear terms in Eqs. (13a) and (13b) reduce to a very simple form for  $\xi=1$  (neutral mode competition), a situation that applies to a single Ne-isotope He-Ne ring laser on line center. In this case the nonlinear coupling is absent so that any amount of linear coupling will dominate. We shall now use the linear two-mode approach to discuss so-called  $\pi$ -phase jumps that were reported recently for exactly this type of laser in the presence of backscattering.<sup>10,13</sup> The terminology refers to sudden jumps (by an amount  $\pi$ ) in the relative phase of the counterpropagating waves in the ring laser. Note that phase jumps were also reported for ring lasers without backscattering.<sup>21</sup> These jumps are completely governed by the nonlinear dynamics and will not be addressed here.

We distinguish here three categories of (backscattering-induced)  $\pi$ -phase jumps, two of which, the “noise-driven jumps” and the “deterministic jumps,” were also discussed by Chyba.<sup>13</sup> The third category, which we call “detuning-driven jumps,” has not been discussed before and is predicted in the present paper.

### A. Noise-driven jumps

Noise-driven jumps were reported<sup>13</sup> for conditions of conservative backscattering [ $\sin\psi=0$  in Eqs. (13a) and

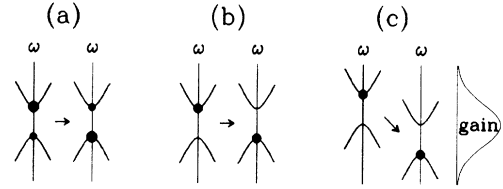


FIG. 3. Pictorial representation of three categories of  $\pi$ -phase jumps in the standing-wave picture. The hyperbola diagrams refer to Fig. 1(b). In (a) the intensity difference of the standing-wave modes changes sign. In (b) and (c) the laser makes a mode hop between the standing-wave normal modes, induced by a change of the backscattering phase (b), or a change in cavity detuning (c). The processes in (a), (b), and (c) are called noise-driven jumps, deterministic jumps, and detuning-driven jumps, respectively.

(13b)] and laser tuning to line center, so that  $\xi=1$ . Under these conditions oscillatory instability was shown to occur in Sec. IV and the behavior of the laser is again most easily understood in the standing-wave picture. Equations (15a) and (15b) show that simultaneous oscillation occurs in two standing-wave modes with frequency difference  $2W$ . As mentioned already, the solution is indifferent to a redistribution of the intensity between the standing waves. Therefore as a result of spontaneous emission and other noise processes, the amplitudes  $F_1$  and  $F_2$  will fluctuate, while the sum of their squares is stabilized, by gain saturation, to the value  $F_1^2 + F_2^2 = a$ . The phase difference between the *standing* waves increases linearly in time, at a rate given by their beat frequency  $2W$ . Although the noise sources will cause some diffusion around the linear increase of the phase, no sudden jumps in this phase are expected.

We will now show that a sudden jump in the phase difference between the *traveling* wave does occur, when the intensity difference of the standing waves,  $F_1^2 - F_2^2$ , changes sign (and thus  $F_1 - F_2$ ) due to the random intensity redistributions. Figure 3(a) shows a pictorial representation of such a process, in which the intensity distribution changes from dominantly in the “upper” mode ( $F_1 > F_2$ ) to dominantly in the “lower” mode ( $F_1 < F_2$ ).

In order to understand that a  $\pi$ -phase jump occurs in this situation, we must return to the traveling-wave picture. In Eqs. (16a) and (16b) the complex traveling-wave amplitudes  $\tilde{E}_1(t)$  and  $\tilde{E}_2(t)$  are expressed in the standing-wave amplitudes  $F_1$  and  $F_2$ . Let us assume that before the phase jump occurs ( $t < t_j$ ), the upper mode is the stronger one ( $F_1 > F_2$ ). As is apparent from Eqs. (16a) and (16b), the evolution of the traveling-wave amplitude  $\tilde{E}_1(t)$  in the complex plane is along an ellipse with semi-major and -minor axes  $(1/\sqrt{2})(F_1 + F_2)$  and  $(1/\sqrt{2})|F_1 - F_2|$ , respectively. For  $\tilde{E}_2(t)$  the axes are interchanged. The ellipses are drawn in Fig. 4(a) for the situation that  $F_1 > F_2$ . The individual phases of the traveling waves ( $\arg\tilde{E}_1$  and  $\arg\tilde{E}_2$ ) will therefore evolve according to the “staircases” in Fig. 4(c) for  $t < t_j$ . The time dependence of the phase difference  $\phi_{21} \equiv \arg\tilde{E}_2 - \arg\tilde{E}_1$  is also given in Fig. 4(c). Note that the series of regular jumps in  $\phi_{21}$  by an amount  $\pi$  for  $t < t_j$  is purely

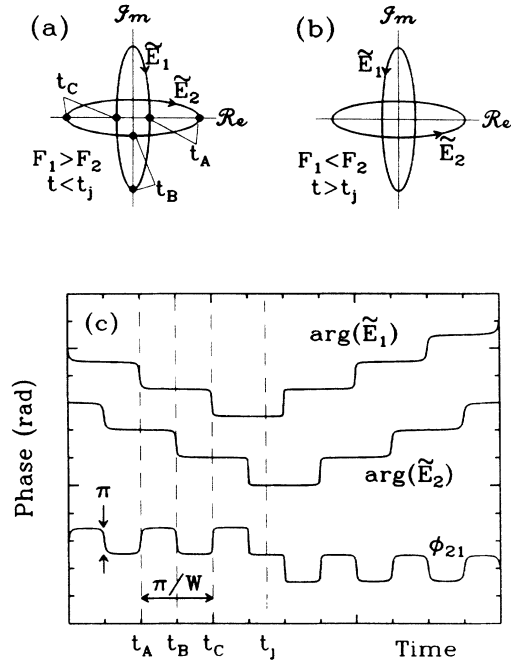


FIG. 4. Evolution of the traveling-wave amplitudes  $\tilde{E}_1(t)$  and  $\tilde{E}_2(t)$  in the complex plane (a) before and (b) after a noise-driven  $\pi$  jump at  $t = t_j$ , with snapshots for  $t = t_{A,B,C} < t_j$ . The ellipses have semi-major and -minor axes  $(F_1 + F_2)/\sqrt{2}$  and  $|F_1 - F_2|/\sqrt{2}$ , respectively. At  $t = t_j$  the sign of  $F_1 - F_2$  changes, so that the sense of circulation around the ellipses is reversed. In (c) the corresponding evolution of the individual phases of  $\tilde{E}_1(t)$  and  $\tilde{E}_2(t)$  and their phase difference  $\phi_{21}$  is given.

deterministic and not of interest here. As mentioned above, the effect of noise is a fluctuation of the standing-wave amplitudes  $F_{1,2}$ , which manifests itself in Fig. 4(a) as a change in ellipticity. Let us assume now that  $F_1$  and  $F_2$  fluctuate in such a way that  $F_1 - F_2$  changes sign at  $t = t_j$ , i.e., we consider a process as shown in Fig. 3(a). As a consequence the ellipses will evolve into line segments at  $t = t_j$  and reappear at  $t > t_j$  [ $F_1 < F_2$ , see Fig. 4(b)]. However, since the sign of  $F_1 - F_2$  is reversed during this process, so is the sense of circulation around the ellipses. The phases of the individual traveling waves thus change, at  $t = t_j$ , from a decreasing into an increasing function of time; see Fig. 4(c). The corresponding trace of the phase difference  $\phi_{21}$  shows an irregular jump by an amount  $\pm\pi$  near  $t = t_j$ .

In conclusion, we find that these noise-driven  $\pi$ -phase jumps arise as an artifact if we choose to work in the traveling-wave basis. If we work instead in the standing-wave basis, i.e., if we use the passive normal modes, we find laser operation in two modes with fluctuating amplitudes.

### B. Deterministic jumps

Deterministic  $\pi$ -phase jumps were reported in experiments on He-Ne ring lasers where the backscattering

phase  $\psi$  was a controllable parameter.<sup>13</sup> We shall show here that these jumps may be interpreted as a mode hop between two standing waves [see Fig. 3(b)], induced by a zero crossing of  $\sin\psi$ . In terms of the discussion of Sec. II, the condition  $\sin\psi \neq 0$  implies that the backscattering is not purely conservative but also contains a dissipative component. Since we associated dissipative coupling with localized losses, we may expect that the standing-wave modes will have different loss and therefore a different threshold gain and a different pump parameter.

In order to see how a mode hop can be induced by adjusting  $\psi$ , let us return to Eqs. (14a) and (14b) and assume  $\sin\psi > 0$ . For the effective pump parameters  $a_1$  and  $a_2$  we find the relation  $a_1 = a + W \sin\psi > a - W \sin\psi = a_2$ . As can be seen from Eq. (14a), for steady-state oscillation we have  $a_1 - |\tilde{F}_1|^2 - |\tilde{F}_2|^2 = 0$ , which directly implies that  $a_2 - |\tilde{F}_1|^2 - |\tilde{F}_2|^2 < 0$ . In other words, mode  $\tilde{F}_2$  will experience loss, so that the stable solution is

$$\tilde{F}_1(t) = e^{-iWt \cos\psi} (a + W \sin\psi)^{1/2}, \quad (17a)$$

$$\tilde{F}_2(t) = 0. \quad (17b)$$

Obviously, for the opposite sign of  $\sin\psi$  the roles of  $F_1$  and  $F_2$  are interchanged, so that the laser responds with a mode hop to a change in sign of  $\sin\psi$ . If the phase difference of the traveling waves is monitored, a jump by an amount  $\pi$  is observed, since the standing-wave modes  $\tilde{F}_1$  and  $\tilde{F}_2$  are  $90^\circ$  out of phase, spatially. During the transient, when both standing waves are present, a beat frequency is observed. We predict another effect that should accompany this phase jump, not reported in Ref. 13, namely a change in frequency of the laser output. The frequency changes by an amount  $\Omega_1 - \Omega_2 = 2W \cos\psi$ , i.e., by an amount  $2W$ , since the mode hop occurs when  $\sin\psi = 0$ .

### C. Detuning-driven jumps

Detuning-driven jumps have, to our knowledge, not been discussed before. We expect such jumps to occur when the He-Ne laser is operated with conservative backscattering, as a response to tuning the cavity through the center of the Doppler-broadened line. These detuning-driven jumps may, just like the deterministic jumps, be identified as mode hops between the two standing-wave normal modes [see Fig. 3(c)]. Actually, when the cavity detuning is a controllable parameter, the detuning-driven jumps are deterministic as well. However, we shall adhere to the present nomenclature in order to maintain the distinction with the deterministic jumps of Sec. V B.

So far all our results were obtained for (single-mode) He-Ne ring lasers tuned to line center leading to a mode-coupling parameter  $\xi = 1$ . This situation reduced the nonlinear effects to the very simple form given in Eqs. (14a) and (14b). When we detune the laser from line center, the nonlinear effects are more complicated. For example, the pump parameter and the self- and cross-saturation coefficients all become complex valued. Menegozzi and Lamb<sup>3</sup> showed theoretically that for an inhomogeneously broadened ring laser with conservative backscattering, detuned from line center, only one stand-

ing wave oscillates, the oscillating mode being determined by the sign of the detuning. Therefore, if we tune the cavity through line center, we expect a mode hop [see Fig. 3(c)]. As a result a  $\pi$  jump is observed in the phase difference between the traveling waves. As in Sec. V B, the phase jump is predicted to be accompanied by a frequency jump of  $2W$ .

We suspect this to be the mechanism underlying the polarization-azimuth flips reported by de Lang and Bouwhuis.<sup>22</sup> In their experiments with a linear 1.15- $\mu\text{m}$  He-Ne laser (i.e., no ring laser) they found that the (linear) polarization of the laser switched from  $E_x$  to  $E_y$  when tuning the laser through the Doppler profile. In order to see the connection with  $\pi$ -phase jumps, it must be realized that the linear two-mode analysis of Sec. II is not at all restricted to describe the coupling between cw and ccw traveling waves in a ring cavity with backscattering. It could equally well be applied to describe the coupling between the opposite circular polarizations of a linear cavity with spurious birefringence. We can then describe the flip of the linear polarization by a  $\pi$  jump in the phase difference between its circular-polarization components.

## VI. EXPERIMENTS

In Sec. IV we interpreted the oscillatory instability in ring lasers with conservative backscattering as a frequency splitting of the normal modes. Although experimental observations of the oscillatory instability have been reported,<sup>2,7-11,13,14</sup> it was, to our knowledge, never observed as a spectral feature. The experiments described in this section are intended to fill this gap and thus support the point of view that the splitting of the passive normal modes, as reported in Refs. 7, 15, and 16, underlies the oscillatory instabilities in the active system. Experiments on phase jumps were reported before<sup>10,11,13</sup> and will not be addressed here.

We performed experiments in two He-Ne ring lasers, both of which were constructed from four mirrors with high reflectivity at  $\lambda=633$  nm. The gain medium was a plasma tube from a Spectra-Physics model 120S He-Ne

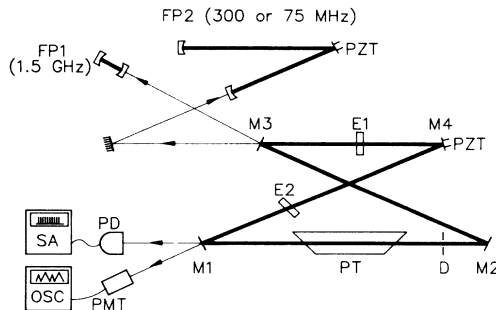


FIG. 5. Experimental setup. M1–M4, mirrors; PT, He-Ne plasma tube; E1, backscattering étalon; E2, étalon for spectral selection (only for single-mode experiment); D, diaphragm; PD, photodiode; PMT, photomultiplier tube; SA, rf spectrum analyzer; OSC, oscilloscope; FP1, confocal 1.5-GHz Fabry-Pérot étalon; FP2, confocal 75- or 300-MHz Fabry-Pérot étalon (see text).

laser. The tube had Brewster windows and was filled with a 9:1 mixture of  $^3\text{He}:^{20}\text{Ne}$  at a tip-off pressure of 3.4 Torr.

The first laser had a length of 1.37 m corresponding to a free spectral range (FSR) of 219 MHz (see Fig. 5). Mirrors M1 and M4 were plane, mirror M2 had a radius of curvature of 6 m and mirror M3 of 1 m. Mirror M4 was mounted on a piezoelectric element to allow for tuning of the cavity. As a backscattering element we used a 1-mm uncoated quartz étalon (E1) perpendicular to the beam, so that the backscattering was always (dominantly) conservative. For spectral selection an extra étalon (E2; 5-mm uncoated quartz) was placed in the beam, slightly tilted to avoid additional backscattering. The laser light coupled out through mirror M3 was analyzed by two confocal Fabry-Pérot interferometers, FP1 and FP2 with a FSR of 1.5 GHz and 300 MHz, respectively. We also monitored the laser light coupled out through mirror M1 in the time domain, using a photomultiplier tube connected to an oscilloscope. The power spectrum of this laser output was measured with an rf spectrum analyzer. The number of oscillating longitudinal modes of the ring laser was monitored with Fabry-Pérot FP1. We used Fabry-Pérot FP2 and the rf spectrum analyzer to detect the backscattering-induced doublet splitting of the individual longitudinal modes. By adjusting étalon E2 the laser could be forced to operate in a single longitudinal mode. Most of the time the laser oscillated in a single-standing-wave mode and no splitting was observed. This is the result to be expected for a He-Ne laser detuned from line center as discussed in Sec. V C. For the two standing waves to oscillate simultaneously, the laser must be tuned to line center. By adjusting étalon E2 and the piezovoltage of M4 we could indeed observe a doublet on Fabry-Pérot FP2 [Fig. 6(a)], and at the same time a single longitudinal mode on FP1 [Fig. 6(b)]. Typical results for the

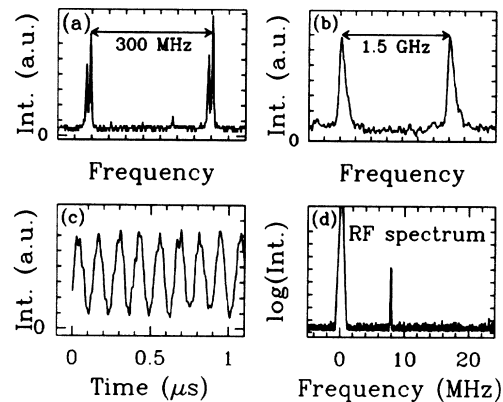


FIG. 6. Experimental results for the spectral and temporal properties of a He-Ne ring laser with conservative backscattering, oscillating in a single longitudinal mode. High- and low-resolution optical spectra obtained with FP1 and FP2 are shown in (a) and (b). The arrows indicate the free spectral range of FP1 and FP2. A longitudinal-mode splitting is visible in (a). The traveling-wave intensity, recorded with the PMT, shows (c) an 8-MHz oscillation and (d) the rf spectrum analyzer reveals the same frequency in the beat spectrum.

corresponding beat note are shown in Figs. 6(c) and 6(d). The photomultiplier signal in Fig. 6(c) shows the oscillatory instability. Only one peak was visible in the rf spectrum, at 8 MHz [Fig. 6(d)]. The mode splitting was not observed when the backscattering étalon E1 was removed. All this provides convincing support for the point of view that the oscillatory instabilities can be interpreted as a splitting of the longitudinal mode of the ring laser, in agreement with Sec. IV.

Although it was assumed throughout this paper that the laser operated in a single longitudinal mode, we also performed experiments in a multimode laser. This laser has a length of 2.97 m, corresponding to a FSR of 101 MHz. The radii of curvature were now 1 m for mirrors M1 and M2, 5 m for mirror M3, and 6 m for mirror M4. In this experiment FP2 was a confocal Fabry-Pérot interferometer with a FSR of 75 MHz. Étalon E2 was removed; as a consequence the ring laser oscillated simultaneously in 5–10 longitudinal modes [see Fig. 7(a)]. Insertion of a 1-mm quartz étalon perpendicular to the beam (E1) produced a splitting of these modes of about 6 MHz [Fig. 7(b)]. In the rf beat spectrum the same mode splitting was visible through the occurrence of 6-MHz

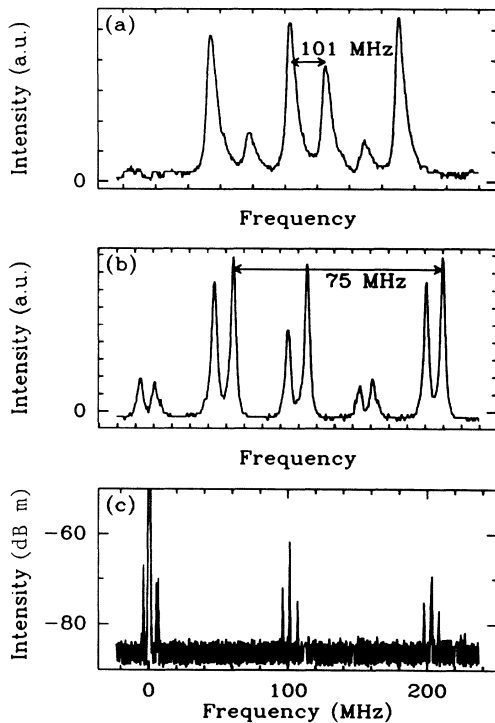


FIG. 7. Spectral and temporal properties of a multimode He-Ne ring laser with conservative backscattering. A low-resolution optical frequency spectrum, obtained with FP1 (free spectral range 1.5 GHz), is shown in (a), where the collection of longitudinal modes appears. The longitudinal mode spacing, i.e., the free spectral range of the laser cavity, is 101 MHz. A high-resolution spectrum, obtained with FP2 (free spectral range 75 MHz), shows (b) the splitting (6 MHz) of the individual modes. (c) The rf spectrum displays 6-MHz sidebands at intermode beats at multiples of the free spectral range of the laser cavity.

sidebands at all intermode beat frequencies [0 and 101 MHz, 202 MHz, . . .; see Fig. 7(c)]. In order to verify the dependence of the splittings on the strength of the backscattering, we replaced the 1-mm quartz étalon (E1) by an étalon with a piezoelectrically adjustable air spacing. The plates of this étalon, a Spectra-Physics model 581B-16, were dielectrically coated. In a separate experiment we established that the effective intensity-reflection coefficient  $R$  could be varied from 0 to 0.73 (at 633 nm) by adjusting the piezovoltage. According to Eq. (10) we may then expect the mode splitting to vary between 0 and 33 MHz. In Fig. 8 we show the mode splitting (determined from the rf beat spectrum) as a function of the piezovoltage, together with the splitting as calculated from Eq. (10). The data show good agreement with theory. The periodicity in Fig. 8 is due to the periodic dependence of  $R$  on the étalon spacing. The period corresponds with a free spectral range of the étalon. The observations show that the linear analysis from Sec. II is apparently also useful in the multimode case. In that case we find the same backscattering-induced longitudinal-mode splitting.

## VII. CONCLUSIONS

The linear formalism presented in this paper provides a convenient framework to discuss backscattering-induced mode coupling in ring lasers in terms of competition between the normal modes of the passive cavity. The approach is useful in those cases where the linear mode coupling due to backscattering dominates the nonlinear coupling due to gain saturation. We have applied the formalism to discuss several effects of backscattering in (rotating) ring lasers. By examining the extreme cases of conservative and dissipative backscattering, the nature of the backscattering was shown to play a crucial role. Dissipative backscattering, associated with localized losses, leads to frequency locking in the mode structure of the passive cavity and will therefore tend to lock the laser

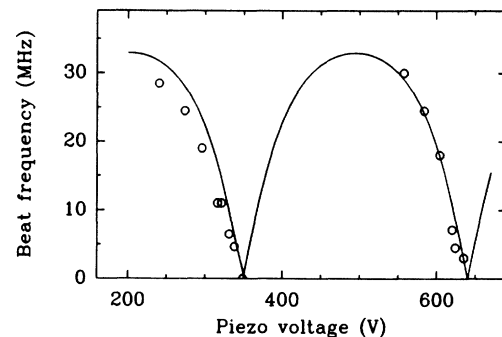


FIG. 8. Behavior of the longitudinal mode splitting in a multimode He-Ne ring laser as the reflection coefficient of an air-spaced backscattering étalon is varied periodically. The étalon spacing depends roughly linearly on the piezovoltage and determines the effective reflection coefficient. The solid curve was calculated with Eq. (10), using a maximum reflection coefficient  $R = 0.73$ . The deviation from the theoretical curve at low voltages is attributed to the nonlinearity of the piezo response.

modes. Conservative backscattering, associated with localized jumps in refractive index, leads to a normal-mode splitting and thus makes oscillatory instability possible. We showed that the latter phenomenon may be seen as a stable operation in the two normal modes of the passive cavity. These are standing-wave modes with a frequency difference proportional to the effective backscattering rate.

The recently reported  $\pi$ -phase jumps in He-Ne ring lasers may be described conveniently in terms of the normal modes of the passive cavity. The noise-driven  $\pi$ -phase jumps were shown to arise as a peculiarity of a description in traveling waves, instead of the normal modes of the passive cavity, which are standing waves. Deterministic jumps can be seen as a mode hop between two standing-wave modes, induced by a change in backscattering phase. We also predicted an alternative type of

phase jump, the detuning-driven jump, which may again be seen as a mode hop between the two standing-wave modes, this time induced by tuning the laser frequency through the Doppler profile. Finally we have presented experimental results on the oscillatory instability, revealing the spectral mode splitting of the individual longitudinal modes, in agreement with the theory developed here.

#### ACKNOWLEDGMENTS

The authors thank T. H. Chyba for communicating his results before publication. This work is part of the research program of the Foundation for Fundamental Research on Matter (FOM) and was made possible by financial support from the Netherlands Organization for Scientific Research (NWO).

<sup>1</sup>F. Aronowitz and R. J. Collins, *J. Appl. Phys.* **41**, 130 (1970).

<sup>2</sup>F. Aronowitz, *Appl. Opt.* **11**, 405 (1972).

<sup>3</sup>L. N. Menegozzi and W. E. Lamb, Jr. *Phys. Rev. A* **8**, 2103 (1973).

<sup>4</sup>S. Stenholm, *Acta Polytech. Scand.* **138**, 165 (1983).

<sup>5</sup>H. A. Haus, H. Statz, and I. W. Smith, *IEEE J. Quantum Electron.* **QE-21**, 78 (1985).

<sup>6</sup>W. W. Chow, J. Gea-Banacloche, L. M. Pedrotti, V. E. Sanders, W. Schleich, and M. O. Scully, *Rev. Mod. Phys.* **57**, 61 (1985).

<sup>7</sup>J. P. Woerdman and R. J. C. Spreeuw, in *Analogies in Optics and Micro-Electronics*, edited by W. van Haeringen and D. Lenstra (Kluwer, Dordrecht, 1990), pp. 135–150.

<sup>8</sup>D. Kühlke, *Acta Phys. Pol. A* **61**, 547 (1982).

<sup>9</sup>W. R. Christian and L. Mandel, *Phys. Rev. A* **34**, 3932 (1986); W. R. Christian, E. C. Gage, and L. Mandel, *Opt. Lett.* **12**, 328 (1987); W. R. Christian and L. Mandel, *J. Opt. Soc. Am. B* **5**, 1406 (1988).

<sup>10</sup>W. R. Christian, T. H. Chyba, E. C. Gage, and L. Mandel, *Opt. Commun.* **66**, 238 (1988).

<sup>11</sup>N. B. Abraham and C. O. Weiss, *Opt. Commun.* **68**, 437 (1988).

<sup>12</sup>L. Pesquera, R. Blanco, and M. A. Rodríguez, *Phys. Rev. A*

**39**, 5777 (1989); L. Pesquera and R. Blanco, *Opt. Commun.* **74**, 102 (1989).

<sup>13</sup>T. H. Chyba, *Phys. Rev. A* **40**, 6327 (1989).

<sup>14</sup>R. Centeno Neelen, R. J. C. Spreeuw, E. R. Eliel, and J. P. Woerdman (unpublished).

<sup>15</sup>D. Lenstra, L. P. J. Kamp, and W. van Haeringen, *Opt. Commun.* **60**, 339 (1986).

<sup>16</sup>R. J. C. Spreeuw, J. P. Woerdman, and D. Lenstra, *Phys. Rev. Lett.* **61**, 318 (1988).

<sup>17</sup>R. J. C. Spreeuw, E. R. Eliel, and J. P. Woerdman, *Opt. Commun.* **75**, 141 (1990).

<sup>18</sup>D. Lenstra and S. H. M. Geurten, *Opt. Commun.* **75**, 63 (1990).

<sup>19</sup>H. Kogelnik and C. V. Shank, *J. Appl. Phys.* **43**, 2327 (1972).

<sup>20</sup>It is shown in Ref. 14 that the rapidly varying terms produce higher harmonics of the beat frequency and thus beat signal distortion. Since the terms are proportional to  $\xi - 1$ , we do not expect these effects in a single Ne-isotope He-Ne ring laser tuned to line center.

<sup>21</sup>L. M. Hoffer, G. L. Lippi, N. B. Abraham, and P. Mandel, *Opt. Commun.* **66**, 219 (1988); C. O. Weiss, N. B. Abraham, and U. Hübner, *Phys. Rev. Lett.* **61**, 1587 (1988).

<sup>22</sup>H. de Lang and G. Bouwhuis, *Phys. Lett.* **19**, 481 (1965).